Published in final edited form as:

Hepatology. 2021 July ; 74(1): 397–410. doi:10.1002/hep.31679.

Farnesoid X Receptor Activation Impairs Liver Progenitor Cell–Mediated Liver Regeneration via the PTEN-PI3K-AKT-mTOR Axis in Zebrafish

Kyounghwa Jung[1], **Minwook Kim**[1], **Juhoon So**[1], **Seung-Hoon Lee**[1], **Sungjin Ko**[1,2], **Donghun Shin**[1]

[1]Department of Developmental Biology, McGowan Institute for Regenerative Medicine, Pittsburgh Liver Research Center, University of Pittsburgh, Pittsburgh, PA;

[2]Division of Experimental Pathology, Department of Pathology, University of Pittsburgh School of Medicine, Pittsburgh, PA.

Abstract

BACKGROUND AND AIMS: Following mild liver injury, pre-existing hepatocytes replicate. However, if hepatocyte proliferation is compromised, such as in chronic liver diseases, biliary epithelial cells (BECs) contribute to hepatocytes through liver progenitor cells (LPCs), thereby restoring hepatic mass and function. Recently, augmenting innate BEC-driven liver regeneration has garnered attention as an alternative to liver transplantation, the only reliable treatment for patients with end-stage liver diseases. Despite this attention, the molecular basis of BEC-driven liver regeneration remains poorly understood.

APPROACH AND RESULTS: By performing a chemical screen with the zebrafish hepatocyte ablation model, in which BECs robustly contribute to hepatocytes, we identified farnesoid X receptor (FXR) agonists as inhibitors of BEC-driven liver regeneration. Here we show that FXR activation blocks the process through the FXR-PTEN (phosphatase and tensin homolog)–PI3K (phosphoinositide 3-kinase)–AKT-mTOR (mammalian target of rapamycin) axis. We found that FXR activation blocked LPC-to-hepatocyte differentiation, but not BEC-to-LPC dedifferentiation. FXR activation also suppressed LPC proliferation and increased its death. These defects were rescued by suppressing PTEN activity with its chemical inhibitor and *ptena*/*b* mutants, indicating PTEN as a critical downstream mediator of FXR signaling in BEC-driven liver regeneration. Consistent with the role of PTEN in inhibiting the PI3K-AKT-mTOR pathway, FXR activation reduced the expression of pS6, a marker of mTORC1 activation, in LPCs of regenerating livers.

ADDRESS CORRESPONDENCE AND REPRINT REQUESTS TO: Sungjin Ko, Ph.D., Division of Experimental Pathology, Department of Pathology, University of Pittsburgh School of Medicine, S451-BST, 200 Lothrop Street, Pittaburgh, PA 15261, sungjin@pitt.edu, Tel.: +1-412-383-7783 or Donghun Shin, Ph.D., Department of Developmental Biology, University of Pittsburgh School of Medicine, 3501 5th Avenue, #5063, Pittsburgh, PA 15260, donghuns@pitt.edu, Tel.: +1-412-624-2144.

Author Contributions: K.J., S.K., and D.S. designed the study. K.J., M.K., J.S., S.L., S.K., and D.S. performed experiments and analyzed data. K.J., S.K., and D.S. interpreted data. D.S. supervised the study. K.J. and D.S. wrote the manuscript. All authors have reviewed and approved the final version of the manuscript.

Supporting Information

Additional Supporting Information may be found at onlinelibrary.wiley.com/doi/10.1002/hep.31679/suppinfo.

Potential conflict of interest: Nothing to report.

Importantly, suppressing PI3K and mTORC1 activities with their chemical inhibitors blocked BEC-driven liver regeneration, as did FXR activation.

CONCLUSIONS: FXR activation impairs BEC-driven liver regeneration by enhancing PTEN activity; the PI3K-AKT-mTOR pathway controls the regeneration process. Given the clinical trials and use of FXR agonists for multiple liver diseases due to their beneficial effects on steatosis and fibrosis, the detrimental effects of FXR activation on LPCs suggest a rather personalized use of the agonists in the clinic.

Although the liver is a highly regenerative organ, chronic liver disease, including cirrhosis, is the 11th leading cause of mortality in the United States.[1] Chronic liver disease usually develops over years due to chronic inflammation and scarring, resulting in end-stage liver disease.[2] Currently, liver transplantation is the only effective treatment for end-stage liver disease[2]; however, the shortage of donor livers and lifelong need for immunosuppressive drugs make this therapy extremely limited.[3,4] A deeper understanding of the molecular mechanisms underlying innate liver regeneration may provide insights into alternative regenerative therapies to augment liver regeneration in patients with end-stage liver disease.

Hepatocytes, which occupy 80% of the liver volume, carry out most liver functions, including metabolism and detoxification. Following injury, hepatocytes proliferate to recover lost liver mass, which is known as hepatocyte-driven liver regeneration.[5] However, if hepatocyte proliferation is compromised or hepatocytes die excessively, as observed in chronic liver disease, hepatocyte replication is not sufficient to restore lost liver mass and function.[6] In this case, biliary epithelial cells (BECs) are activated and give rise to hepatocytes, called BEC-driven liver regeneration. Zebrafish[7,8] and mouse[9–12] studies with severe liver injury models have revealed the significant contribution of BECs to hepatocytes and functional recovery. Moreover, human studies with cirrhotic livers showed that a large percentage of hepatocytes in the regressed liver appear to originate from BECs,[13] suggesting the importance of BEC-driven liver regeneration in cirrhosis regression.

In the zebrafish liver injury model, *Tg(fabp10a:CFP [cyan fluorescent protein]–NTR [nitroreductase])*^{s931}, BECs robustly and rapidly contribute to hepatocytes within a day following near-total ablation of hepatocytes.[7] Given this robustness and rapidity, we have successfully used this model for chemical screening to identify small molecules that affect BEC-driven liver regeneration.[14] Through the screening, we have reported the essential roles of BET proteins,[14] Hdac1[15] and Kdm1,[15] in BEC-driven liver regeneration. We also found that treatment with the farnesoid X receptor (FXR) agonist GW4064 greatly reduced the size of regenerating livers,[14] suggesting a negative effect of FXR activation on BEC-driven liver regeneration. As a nuclear receptor, FXR signaling is known for its beneficial effects on alleviating steatosis, fibrosis, and insulin resistance,[16,17] and on promoting hepatocyte-driven liver regeneration.[18,19] These beneficial effects are in stark contrast to the negative effect of FXR activation on BEC-driven liver regeneration. Given the clinical trials of FXR agonists for treating multiple liver diseases, including nonalcoholic steatohepatitis,[20] and their clinical use as a drug for primary biliary cirrhosis,[21] we provide the evidence of the detrimental effect of FXR activation on BEC-driven

liver regeneration and its underlying molecular mechanism, which will advocate a rather personalized use of FXR agonists in the clinic.

Materials and Methods

ZEBRAFISH LINES

All zebrafish experiments were performed under the approval of the Institutional Animal Use and Care Committee at the University of Pittsburgh. Embryos and adult fish were raised and maintained under standard laboratory conditions.[22] We used *fxr*^{pt667}, *ptena*^{hu1864}, and *ptenb*^{hu1435} mutant and the following transgenic lines: *Tg(fabp10a:CFP-NTR)*^{s931}, *Tg(Tp1:H2B-mCherry)*^{s939}, *Tg(Tp1:VenusPEST)*^{s940}, *Tg(fabp10a: DsRed)*^{gz15}, *Tg(fabp10a:rasGFP)*^{s942}, and *Tg(fabp10a: pt-β-catenin)*^{s704}. Their full and official names are listed in Supporting Table S1.

GENERATION OF THE *fxr*^{pt667} MUTANT LINE

The CRISPR/Cas9-mediated genome editing technology[23] was used to make the *fxr* mutant line. Briefly, the 5′-GGGTGGTTTTGATAATGAGCTGG-3′ (with protospacer adjacent motif sequence underlined) region in the second coding exon of *nr1h4* was targeted. One or 2 nL of a mixture containing single-guide RNA (7 ng/μL) and Cas9 messenger RNA (250 ng/μL) was injected into 1 cell–stage embryos. Mutations were initially identified by PCR following T7 endonuclease or *AluI* digestion with a forward (5′-ATATTCTGGCAGAGCAGAACAGTCC-3′) and a reverse (5′-AACACCAGCAAAAATACAAAAAGGATTCACCTTTACATCCTTCACAAGTG-3′) primer pair. F1 fish containing a 13-b deletion mutation was selected to establish the mutant line. For easier genotyping, a forward (5′-TGGTACTCTCCGTCCGCCATG-3′) and a reverse (5′-GTTGTAGTGATACCCTGAGGCT-3′) primer pair were used for PCR; the wild-type and mutant allele displayed 195-bp and 182-bp PCR products, respectively.

HEPATOCYTE ABLATION USING *Tg(fabp10a:CFP-NTR)* LARVAE

To ablate hepatocytes, *Tg(fabp10a:CFP-NTR)* larvae were treated with 10 mM metronidazole (Mtz) in egg water supplemented with 0.2% dimethyl sulfoxide (DMSO) and 0.2 mM 1-phenyl-2-thiourea from 3.5 to 5 days post-fertilization (dpf) for 36 hours, as previously described.[24]

COMPOUND TREATMENTS

The following compounds were used: FXR agonists (1 μM GW4064, 4 μM obeticholic acid (OCA), and 10 nM tropifexor), a phosphatase and tensin homolog (PTEN) inhibitor (2 μM SF1670), a phosphoinositide 3-kinase (PI3K) inhibitor (10 μM LY294002), a mammalian target of rapamycin (mTOR) C1 inhibitor (10 μM rapamycin), and an FXR antagonist (10 μM DY268).

QUANTIFICATION OF Bhmt+ LIVER AREA

Confocal images of anti-Bhmt immunostaining and *fabp10a*:CFP intrinsic fluorescence were used to quantify the Bhmt$^+$ liver area. Both Bhmt$^+$ and *fabp10a*:CFP$^+$ areas in the liver were calculated by ImageJ, and the former area was divided by the latter.

Additional methods are available in the Supporting Information.

Results

FXR ACTIVATION IMPAIRS BEC-DRIVEN LIVER REGENERATION

To better understand the molecular mechanisms underlying BEC-driven liver regeneration, we had previously performed a chemical screen using our zebrafish liver injury model, *Tg(fabp10a:CFP-NTR)*^{s931}, which expresses CFP-NTR fusion proteins specifically in hepatocytes.[7] The NTR enzyme metabolizes nontoxic Mtz into a cytotoxic drug; thus, Mtz treatment ablates only hepatocytes in *Tg(fabp10a:CFP-NTR)* fish. Through this screen, we identified GW4064 as a potent inhibitor of BEC-driven liver regeneration. GW4064 treatment from ablation 0 hour (A0h), but not from A36h or regeneration 0 hour (R0h), onward greatly reduced the size of regenerating livers (Fig. 1A). Its treatment from A18h also produced the same phenotype as A0h treatment (Supporting Fig. S1). We first examined whether *fxr* (official name: *nr1h4*) is expressed in the regenerating liver. Indeed, *fxr* was strongly expressed in the regenerating liver at R6h as well as the uninjured normal liver at 5 dpf (Fig. 1B, arrows). Double labeling with *fxr in situ* hybridization and Anxa4, a BEC/liver progenitor cell (LPC) marker, immunostaining revealed *fxr* expression in LPCs and BECs (Fig. 1C, arrowheads) as well as hepatocytes. Altogether, these data strongly suggest the negative effect of FXR activation on BEC-driven liver regeneration.

FXR ACTIVATION BLOCKS DIFFERENTIATION OF LPCs INTO HEPATOCYTES, BUT NOT DEDIFFERENTIATION OF BECs INTO LPCs

There are three main steps in BEC-driven liver regeneration: (1) dedifferentiation of BECs into LPCs; (2) differentiation of LPCs into hepatocytes; and (3) the proliferation of BEC-derived cells.[7] We determined which step was impaired by FXR activation. To assess the dedifferentiation step, we examined the expression of Prox1 and *fabp10a*:rasGFP, which are induced in LPCs,[7,25] in regenerating livers at R6h. We also used a Notch reporter line, *Tg(Tp1:H2B-mCherry)*^{s939}, which expresses very stable H2B-mCherry fusion proteins in BECs, to mark BECs and BEC-derived cells. The GW4064-treated regenerating livers exhibited strong Prox1 expression in all *Tp1*:H2B-mCherry$^+$ (BEC-derived) cells at R6h, as did control regenerating livers (Fig. 2A). Moreover, *fabp10a*:rasGFP was normally induced in BEC-derived cells at R6h (Fig. 2B), indicating that dedifferentiation of BECs into LPCs is not blocked by FXR activation.

Intriguingly, the expression of Hnf4a (hepatocyte nuclear factor 4a), a hepatoblast/hepatocyte marker, was barely detected in GW4064-treated regenerating livers at R6h (Fig. 2B). Because Hnf4a is a master regulator of hepatocyte differentiation,[26] the lack of Hnf4a expression suggests a defect in differentiation of LPCs into hepatocytes. Indeed, the expression of multiple hepatocyte markers (Bhmt, Hnf4a, *cp*, *gc*, *tdo2a*, and *cyp7a1a*) was

greatly reduced in GW4064-treated regenerating livers compared with control regenerating livers (Fig. 3A–D). The expression of LPC/BEC markers gradually disappears during the conversion of BECs to hepatocytes; eventually, it is not detected in BEC-derived hepatocytes in regenerating livers at R24h.[7] Consistent with impaired LPC-to-hepatocyte differentiation by FXR activation, the expression of the LPC/BEC marker Alcam was sustained in all BEC-derived cells in GW4064-treated regenerating livers at R24h (Fig. 3E). We also used another Notch reporter line, *Tg(Tp1:VenusPEST)*^{s940}, which expresses unstable VenusPEST fusion proteins. Because of the short half-life of VenusPEST, this line reveals cells with active Notch signaling (i.e., BECs and LPCs), but not hepatocytes, in regenerating livers.[7] *Tp1:*VenusPEST was restrictively expressed only in BECs in control regenerating livers at R24h, whereas it was expressed in all BEC-derived cells in GW4064-treated regenerating livers (Fig. 3E). Altogether, these data reveal that FXR activation blocks LPC-to-hepatocyte differentiation.

EFFECT OF GW4064 ON BEC-DRIVEN LIVER REGENERATION IS MEDIATED BY FXR ACTIVATION

Although GW4064 is a highly selective FXR agonist, it is still possible that the effect of GW4064 on BEC-driven liver regeneration may not be mediated by FXR activation. To test this possibility, we generated an *fxr* mutant line with 13-bp deletion in its second coding exon using CRISPR/Cas9-mediated genome editing (Fig. 4A). Although NTR/Mtz-mediated hepatocyte ablation did not work well in $fxr^{-/-}$ mutants (no or partial loss of hepatocytes), it worked well in $fxr^{+/-}$ mutants as in wild-type larvae (near total loss of hepatocytes). Importantly, 1 μM GW4064 treatment blocked BEC-driven liver regeneration significantly less in $fxr^{+/-}$ than wild-type siblings, as assessed by Bhmt expression and liver size (Fig. 4B). Consistent with this dosage effect, 0.5 μM GW4064 treatment did not impair BEC-driven liver regeneration in wild-type larvae (Fig. 4C). Moreover, we tested two other FXR agonists used in clinical trials: OCA[21] and tropifexor.[27] Both OCA and tropifexor treatments blocked BEC-driven liver regeneration, as did GW4064 (Fig. 4D). Altogether, these data support the negative effect of FXR activation on BEC-driven liver regeneration.

We next investigated whether reducing FXR signaling could promote BEC-driven liver regeneration. Because liver regeneration occurs so rapidly and robustly in the NTR/Mtz-mediated hepatocyte ablation model, this model may not be suitable for identifying compounds or conditions that promote the regeneration. In fact, there was no significant difference in liver size and Bhmt expression between wild-type and $fxr^{+/-}$-regenerating larvae at R24h (Fig. 4B). Treatment with the FXR antagonist DY268[28] also did not result in any difference in liver size or Bhmt expression (data not shown). Thus, we used another zebrafish model for LPC-mediated liver regeneration, *Tg(fabp10a:pt-β-catenin)*^{s704}, in which LPCs gradually and slowly differentiate into hepatocytes.[29] In this model, hepatocyte-specific expression of the stable form of mutated β-catenin (pt-β-catenin) elicits oncogene-induced senescence and cell death in hepatocytes, followed by dedifferentiation of pre-existing hepatocytes and BECs into LPCs. Then, these LPCs gradually differentiate into hepatocytes over 7 days. Both $fxr^{+/-}$ and $fxr^{-/-}$ mutants displayed more $Bhmt^{+}$ hepatocytes in 14-dpf *Tg(fabp10a:pt-β-catenin)* livers compared with their wild-type siblings (Supporting Fig. S2A). Moreover, DY268 treatment from 13 dpf to 15 dpf increased

Bhmt expression in 15-dpf *Tg(fabp10a:pt-β-catenin)* livers compared with DMSO treatment (Supporting Fig. S2B). These FXR suppression data further support the negative effect of FXR activation on BEC-driven liver regeneration.

FXR ACTIVATION REDUCES THE PROLIFERATION OF BEC-DERIVED CELLS AND INCREASES THEIR DEATH

Given the reduced liver size in GW4064-treated regenerating larvae at R6h (Fig. 2A) and R24h (Fig. 1A and Supporting Fig. S1), we examined proliferation and cell death in regenerating livers at R6h. The proliferation of BEC-derived cells was significantly reduced in GW4064-treated regenerating livers compared with control regenerating livers, as assessed by 5-ethynyl-2′-deoxyuridine labeling (Fig 5A). The expression of *pcna*, a proliferating cell nuclear antigen was also significantly reduced in GW4064-treated regenerating livers (Fig. 5B). In addition to this impaired proliferation, cell death was observed only in GW4064-treated regenerating livers, as assessed by active Caspase-3 expression (Fig. 5C). Among four pro-apoptotic genes (*bida*, *fas*, *tp53*, and *cdkn1a*), whose expression we examined using quantitative PCR, *fas* expression was significantly increased in GW4064-treated regenerating livers compared with control regenerating livers (Fig. 5D). Albeit not significant, the expression of *bida*, *tp53*, and *cdkn1a* showed an increasing tendency, whereas the expression of the anti-apoptotic gene *bcl2a* showed a decreasing tendency, in GW4064-treated regenerating livers compared with control regenerating livers (Fig. 5D). Altogether, these data indicate that FXR activation represses the proliferation of BEC-derived cells and increases their death during BEC-driven liver regeneration.

PTEN SUPPRESSION RESCUES DEFECTS IN BEC-DRIVEN LIVER REGENERATION OBSERVED IN GW4064-TREATED REGENERATING LARVAE

The effects of FXR agonists on BEC-driven liver regeneration are quite similar to their effects on liver cancers: reduction of proliferation and induction of cell death.[30,31] Given this similarity, we hypothesized that a key downstream mediator that relays FXR activation to impaired BEC-driven liver regeneration would be among the downstream mediators of FXR activation in tumor settings. To determine the molecular mechanism by which FXR activation impairs BEC-driven liver regeneration, we tested the downstream mediators mostly identified from tumor studies, including PTEN,[32] SOCS3/STAT3,[33] Wnt/β-catenin,[34] p62/SQSTM1,[35] p53,[36] autophagy,[37] and MYC.[38] Among these candidates, we identified PTEN as the critical mediator of FXR activation in BEC-driven liver regeneration. Reducing PTEN phosphatase activity with the PTEN inhibitor SF1670[39] in GW4064-treated regenerating larvae partially, but significantly, rescued the defects in (1) liver size, (2) LPC-to-hepatocyte differentiation, and (3) the proliferation and death of BEC-derived cells (Fig. 6A and Supporting Fig. S3A,B). We further confirmed the findings from SF1670 treatment with *pten* mutants. In the zebrafish genome, there are two *pten* genes: *ptena* and *ptenb*. Their double, but not single, homozygous mutants die around 5 dpf with pleiotropic defects,[40] indicating functional redundancy between *ptena* and *ptenb*. NTR/Mtz-mediated hepatocyte ablation and subsequent BEC-driven liver regeneration occurred normally in $ptena^{hu1864}$ and $ptenb^{hu1435}$ mutants (Supporting Fig. S4). Importantly, the defects in BEC-driven liver regeneration observed in GW4064-treated regenerating larvae were significantly rescued in either *ptena* or *ptenb* heterozygous mutants

(Fig. 6B,C and Supporting Fig. S5A,B). Intriguingly, *ptena* or *ptenb* homozygous mutants exhibited no rescue in LPC-to-hepatocyte differentiation and less rescue in liver size than the heterozygous mutants (Fig. 6B,C). These mutant data suggest that among the four copies of the *pten* genes, the deletion of only one copy rescues the defect in LPC-to-hepatocyte differentiation. Consistent with this speculation, *ptena;ptenb* double heterozygous mutants exhibited no rescue in LPC-to-hepatocyte differentiation (Supporting Fig. S5C). Altogether, these data demonstrate that FXR activation impairs BEC-driven liver regeneration, in part, through enhanced PTEN activity.

INHIBITION OF PI3K AND mTOR SIGNALING IMPAIRS BEC-DRIVEN LIVER REGENERATION, AS DOES FXR ACTIVATION

As a phosphatase, PTEN dephosphorylates phosphatidylinositol (3,4,5)-trisphosphate into phosphatidylinositol (4,5)-bisphosphate, thereby suppressing PI3K-AKT signaling.[41] Given that FXR overexpression in liver cancer cells blocks their growth by suppressing mTOR signaling,[42] we hypothesized that enhanced PTEN activity by FXR activation in the regenerating liver suppresses the PI3K-AKT-mTOR pathway, thereby impairing BEC-driven liver regeneration. To test this hypothesis, we first examined whether FXR activation would reduce mTOR signaling in the regenerating liver by assessing the expression of pS6, a reliable marker for mTORC1 activation.[43] pS6 expression was clearly detected in nearly all BEC-derived LPCs at R6h and hepatocytes at R24h (Fig. 7A), indicating active mTOR signaling in the regenerating liver, specifically in BEC-derived cells. As expected, this pS6 expression was greatly reduced in GW4064-treated regenerating larvae (Fig. 7A), indicating that FXR activation suppresses mTOR signaling during BEC-driven liver regeneration. Using small molecules that inhibit the PI3K-AKT-mTOR pathway, we next tested whether suppressing this pathway would block BEC-driven liver regeneration, as observed in GW4064-treated regenerating livers. LY294002 (PI3K inhibitor, 10 μM) and rapamycin (mTORC1 inhibitor, 10 μM) treatments greatly reduced the size of regenerating livers and the hepatic expression of Bhmt and *fabp10a*:CFP at R24h (Fig. 7B–E) and the proliferation of BEC-derived cells at R6h (Supporting Fig. S6A), as observed in GW4064-treated regenerating livers. The treatments also induced the death of BEC-derived cells at R6h, although not significantly (Supporting Fig. S6B). Altogether, these data indicate the positive role of the PI3K-AKT-mTOR pathway in BEC-driven liver regeneration and suggest that FXR activation impairs BEC-driven liver regeneration through the FXR-PTEN-PI3K-AKT-mTOR axis.

Discussion

In this study, using the zebrafish model of BEC-driven liver regeneration, we provide the negative effects of FXR activation on BEC-driven liver regeneration: (1) blocking LPC-to-hepatocyte differentiation, (2) reducing proliferation of LPCs, and (3) increasing death of LPCs (Supporting Fig. S8). Given the beneficial effects of FXR activation on hepatocyte-driven liver regeneration,[19] steatosis, fibrosis, and insulin resistance,[16,17] these negative effects are rather unexpected and surprising. We moreover provide the molecular mechanism by which FXR activation impairs BEC-driven liver regeneration: FXR activation enhances PTEN activity, thereby impairing the process. Finally, we provide the crucial role of the

PI3K-AKT-mTOR pathway in BEC-driven liver regeneration. Altogether, we present the role of the FXR-PTEN-PI3K-AKT-mTOR axis in regulating BEC-driven liver regeneration (Supporting Fig. S8).

The regeneration process in the zebrafish hepatocyte ablation model is rapid, robust, and synchronous. Compared with rodent models of BEC-driven liver regeneration,[10] these features make the zebrafish model ideal for chemical screening, which led us to identify FXR agonists as a potent inhibitor of BEC-driven liver regeneration. The features also make it possible to delineate the process of BEC-driven liver regeneration in great detail, which permitted us to reveal that FXR activation did not impair BEC-to-LPC dedifferentiation but blocked LPC-to-hepatocyte differentiation. Moreover, compound treatment during different time windows allowed us to identify a critical time window during which FXR activation affects BEC-driven liver regeneration. GW4064 treatment from A18h but not A36h (R0h) onward impaired BEC-driven liver regeneration, indicating the duration between A18h and A36h, but not after A36h (R0h), as a critical time window for the negative effects of FXR activation on the regeneration. In addition to the hepatocyte ablation model, we recently established another zebrafish model for BEC/LPC-driven liver regeneration, in which LPCs gradually differentiate into hepatocytes over 7 days.[29] Because of the relatively slow differentiation of LPCs, this model is suitable for identifying small molecules or conditions that promote LPC-to-hepatocyte differentiation. Using this model, we could show that FXR suppression promoted LPC-to-hepatocyte differentiation. This complementary use of the two zebrafish models further strengthens the usefulness of the zebrafish system for elucidating the molecular mechanisms of BEC-driven liver regeneration.

FXR signaling promotes hepatocyte-driven liver regeneration by promoting the proliferation of hepatocytes in mouse liver injury models, including partial hepatectomy[18] and the injection of hepatotoxins, such as CCl_4 [44] and acetaminophen.[45] We also observed the positive effect of FXR activation on hepatocyte-driven liver regeneration in zebrafish larvae treated with acetaminophen (Supporting Fig. S7A), in which pre-existing hepatocytes, but not BECs, contribute to regenerating hepatocytes.[5] Moreover, we observed the positive effect of FXR activation on liver growth in zebrafish larvae without liver damage (Supporting Fig. S7B). In stark contrast, FXR signaling impairs BEC-driven liver regeneration by suppressing the proliferation of LPCs, enhancing their death and blocking their differentiation. These opposite effects of FXR signaling between hepatocyte-driven and BEC-driven liver regeneration can be explained by the difference in cell types affected. Hepatocytes are affected in the former, whereas LPCs are affected in the latter. LPCs dedifferentiated from BECs or hepatocytes obtain progenitor features, including proliferation, and cancer cells often acquire such progenitor features, raising a similarity between cancer cells and LPCs. Supporting this notion, we previously reported that inhibitors of BET bromodomain proteins, which suppress the growth of various cancer cells and therefore are in clinical trials, impair BEC-driven liver regeneration.[14] Moreover, FXR activation suppresses tumor growth by inhibiting cell proliferation and inducing cell death in multiple cancer cells, including liver carcinoma.[46,47] This anticancer effect of FXR activation is very similar to the effect of FXR activation on BEC-driven liver regeneration. Based on this similarity, we discovered that FXR activation impairs the regeneration by

enhancing PTEN activity. In a prostate adenocarcinoma cell line, FXR activation inhibits its proliferation through the same mechanism.[32]

Given that enhanced PTEN activity suppresses PI3K-AKT-mTOR signaling,[48] we automatically evaluated the role of the PI3K-AKT-mTOR pathway in BEC-driven liver regeneration. It was recently reported that in zebrafish, mTOR signaling plays an essential role in BEC-driven liver regeneration,[49] and that in mice, mTORC1 positively regulates LPC proliferation.[50] Indeed, FXR activation greatly reduced the level of mTORC1 activation in LPCs of the regenerating livers. Importantly, PI3K or mTORC1 inhibition impaired BEC-driven liver regeneration, as did FXR activation. These data suggest that enhanced PTEN activity by FXR activation impairs BEC-driven liver regeneration by suppressing PI3K-AKT-mTORC1 signaling.

In summary, we provide the detrimental effects of FXR activation on BEC-driven liver regeneration, specifically on LPCs, and demonstrate that the effects are mediated by the FXR-PTEN-PI3K-AKT-mTOR axis. Our findings suggest a rather personalized use of FXR agonists for treating patients with chronic liver diseases in the clinic.

Supplementary Material

Refer to Web version on PubMed Central for supplementary material.

Acknowledgment:

We thank Jeroen den Hertog for the *ptena* and *ptenb* mutant fish, Jinrong Peng for the anti-Bhmt antibodies, Neil Hukriede and Michael Tsang for the discussion, and Angie Kim for the critical reading of the manuscript.

Supported by the National Institutes of Health (NIH) (DK101426 and DK116993) and the NIH/National Institute of Diabetes and Digestive and Kidney Disease (P30DK120531).

Abbreviations:

BEC	biliary epithelial cell
CFP	cyan fluorescent protein
DMSO	dimethyl sulfoxide
dpf	days post-fertilization
FXR	farnesoid X receptor
Hnf4a	hepatocyte nuclear factor 4a
LPC	liver progenitor cell
mTOR	mammalian target of rapamycin
Mtz	metronidazole
ns	not significant

NTR	nitroreductase
OCA	obeticholic acid
PI3K	phosphoinositide 3-kinase
PTEN	phosphatase and tensin homolog

REFERENCES

1). Heron M Deaths: leading causes for 2017. Natl Vital Stat Rep 2019;68:1–77.

2). Potosek J, Curry M, Buss M, Chittenden E. Integration of palliative care in end-stage liver disease and liver transplantation. J Palliat Med 2014;17:1271–1277. [PubMed: 25390468]

3). Annual Data Report of the US Organ Procurement and Transplantation Network (OPTN) and the Scientific Registry of Transplant Recipients (SRTR). Introduction. Am J Transplant 2013;13(Suppl. 1):8–10. [PubMed: 23237694]

4). Londono MC, Rimola A, O'Grady J, Sanchez-Fueyo A. Immunosuppression minimization vs. complete drug withdrawal in liver transplantation. J Hepatol 2013;59:872–879. [PubMed: 23578883]

5). Fausto N, Campbell JS, Riehle KJ. Liver regeneration. Hepatology 2006;43:S45–S53. [PubMed: 16447274]

6). Miyajima A, Tanaka M, Itoh T. Stem/progenitor cells in liver development, homeostasis, regeneration, and reprogramming. Cell Stem Cell 2014;14:561–574. [PubMed: 24792114]

7). Choi TY, Ninov N, Stainier DY, Shin D. Extensive conversion of hepatic biliary epithelial cells to hepatocytes after near total loss of hepatocytes in zebrafish. Gastroenterology 2014;146:776–788. [PubMed: 24148620]

8). He J, Lu H, Zou Q, Luo L. Regeneration of liver after extreme hepatocyte loss occurs mainly via biliary transdifferentiation in zebrafish. Gastroenterology 2014;146:789–800.e788. [PubMed: 24315993]

9). Raven A, Lu WY, Man TY, Ferreira-Gonzalez S, O'Duibhir E, Dwyer BJ, et al. Cholangiocytes act as facultative liver stem cells during impaired hepatocyte regeneration. Nature 2017;547:350–354. [PubMed: 28700576]

10). Deng X, Zhang X, Li W, Feng RX, Li L, Yi GR, et al. Chronic liver injury induces conversion of biliary epithelial cells into hepatocytes. Cell Stem Cell 2018;23:114–122.e113. [PubMed: 29937200]

11). Manco R, Clerbaux L-A, Verhulst S, Bou Nader M, Sempoux C, Ambroise J, et al. Reactive cholangiocytes differentiate into proliferative hepatocytes with efficient DNA repair in mice with chronic liver injury. J Hepatol 2019;70:1180–1191. [PubMed: 30794890]

12). Russell JO, Lu WY, Okabe H, Abrams M, Oertel M, Poddar M, et al. Hepatocyte-specific beta-catenin deletion during severe liver injury provokes cholangiocytes to differentiate into hepatocytes. Hepatology 2019;69:742–759. [PubMed: 30215850]

13). Stueck AE, Wanless IR. Hepatocyte buds derived from progenitor cells repopulate regions of parenchymal extinction in human cirrhosis. Hepatology 2015;61:1696–1707. [PubMed: 25644399]

14). Ko S, Choi TY, Russell JO, So J, Monga SPS, Shin D. Bromodomain and extraterminal (BET) proteins regulate biliary-driven liver regeneration. J Hepatol 2016;64:316–325. [PubMed: 26505118]

15). Ko S, Russell JO, Tian J, Gao CE, Kobayashi M, Feng R, et al. Hdac1 Regulates differentiation of bipotent liver progenitor cells during regeneration via Sox9b and Cdk8. Gastroenterology 2019;156:187–202.e114. [PubMed: 30267710]

16). Vallim TQD, Tarling EJ, Edwards PA. Pleiotropic roles of bile acids in metabolism. Cell Metab 2013;17:657–669. [PubMed: 23602448]

17). Zhang S, Wang J, Liu Q, Harnish DC. Farnesoid X receptor agonist WAY-362450 attenuates liver inflammation and fibrosis in murine model of non-alcoholic steatohepatitis. J Hepatol 2009;51:380–388. [PubMed: 19501927]

18). Huang W, Ma K, Zhang J, Qatanani M, Cuvillier J, Liu J, et al. Nuclear receptor-dependent bile acid signaling is required for normal liver regeneration. Science 2006;312:233–236. [PubMed: 16614213]

19). Zhang L, Wang Y-D, Chen W-D, Wang X, Lou G, Liu N, et al. Promotion of liver regeneration/repair by farnesoid X receptor in both liver and intestine in mice. Hepatology 2012;56: 2336–2343. [PubMed: 22711662]

20). Ali AH, Carey EJ, Lindor KD. Recent advances in the development of farnesoid X receptor agonists. Ann Transl Med 2015;3:5. [PubMed: 25705637]

21). Nevens F, Andreone P, Mazzella G, Strasser SI, Bowlus C, Invernizzi P, et al. A placebo-controlled trial of obeticholic acid in primary biliary cholangitis. N Engl J Med 2016;375:631–643. [PubMed: 27532829]

22). Westerfield M The Zebrafish Book: A Guide for the Laboratory Use of Zebrafish (Danio Rerio). Eugene, OR: University of Oregon Press; 2000.

23). Chang N, Sun C, Gao L, Zhu D, Xu X, Zhu X, et al. Genome editing with RNA-guided Cas9 nuclease in zebrafish embryos. Cell Res 2013;23:465–472. [PubMed: 23528705]

24). Choi TY, Khaliq M, Ko S, So J, Shin D. Hepatocyte-specific ablation in zebrafish to study biliary-driven liver regeneration. J Vis Exp 2015;99:e52785.

25). Choi TY, Khaliq M, Tsurusaki S, Ninov N, Stainier DYR, Tanaka M, et al. Bone morphogenetic protein signaling governs biliary-driven liver regeneration in zebrafish through tbx2b and id2a. HEPATOLOGY 2017;66:1616–1630. [PubMed: 28599080]

26). DeLaForest A, Di Furio F, Jing R, Ludwig-Kubinski A, Twaroski K, Urick A, et al. HNF4A regulates the formation of hepatic progenitor cells from human iPSC-derived endoderm by facilitating efficient recruitment of RNA Pol II. Genes (Basel) 2018;10:21.

27). Tully DC, Rucker PV, Chianelli D, Williams J, Vidal A, Alper PB, et al. Discovery of tropifexor (LJN452), a highly potent non-bile acid FXR agonist for the treatment of cholestatic liver diseases and nonalcoholic steatohepatitis (NASH). J Med Chem 2017;60:9960–9973. [PubMed: 29148806]

28). Sissung TM, Huang PA, Hauke RJ, McCrea EM, Peer CJ, Barbier RH, et al. Severe hepatotoxicity of mithramycin therapy caused by altered expression of hepatocellular bile transporters. Mol Pharmacol 2019;96:158–167. [PubMed: 31175181]

29). So J, Kim M, Lee SH, Ko S, Lee DA, Park H, et al. Attenuating the EGFR-ERK-SOX9 axis promotes liver progenitor cell-mediated liver regeneration in zebrafish. Hepatology 2021;73:1494–1508. [PubMed: 32602149]

30). Huang XF, Zhao WY, Huang WD. FXR and liver carcinogenesis. Acta Pharmacol Sin 2015;36:37–43. [PubMed: 25500874]

31). Jiang Y, Iakova P, Jin J, Sullivan E, Sharin V, Hong I-H, et al. Farnesoid X receptor inhibits gankyrin in mouse livers and prevents development of liver cancer. Hepatology 2013;57:1098–1106. [PubMed: 23172628]

32). Liu J, Tong SJ, Wang X, Qu LX. Farnesoid X receptor inhibits LNcaP cell proliferation via the upregulation of PTEN. Exp Ther Med 2014;8:1209–1212. [PubMed: 25187826]

33). Guo F, Xu Z, Zhang Y, Jiang P, Huang G, Chen S, et al. FXR induces SOCS3 and suppresses hepatocellular carcinoma. Oncotarget 2015;6:34606–34616. [PubMed: 26416445]

34). Wolfe A, Thomas A, Edwards G, Jaseja R, Guo GL, Apte U. Increased activation of the Wnt/beta-catenin pathway in spontaneous hepatocellular carcinoma observed in farnesoid X receptor knockout mice. J Pharmacol Exp Ther 2011;338:12–21. [PubMed: 21430080]

35). Haga S, Yimin, Ozaki M. Relevance of FXR-p62/SQSTM1 pathway for survival and protection of mouse hepatocytes and liver, especially with steatosis. BMC Gastroenterol 2017;17:9. [PubMed: 28086800]

36). Fujino T, Sakamaki R, Ito H, Furusato Y, Sakamoto N, Oshima T, et al. Farnesoid X receptor regulates the growth of renal adenocarcinoma cells without affecting that of a normal renal cell-derived cell line. J Toxicol Sci 2017;42:259–265. [PubMed: 28496032]

37). Alasmael N, Mohan R, Meira LB, Swales KE, Plant NJ. Activation of the Farnesoid X-receptor in breast cancer cell lines results in cytotoxicity but not increased migration potential. Cancer Lett 2016;370:250–259. [PubMed: 26545738]

38). Takahashi S, Tanaka N, Fukami T, Xie C, Yagai T, Kim D, et al. Role of farnesoid X receptor and bile acids in hepatic tumor development. Hepatol Commun 2018;2:1567–1582. [PubMed: 30556042]

39). Rosivatz E, Matthews JG, McDonald NQ, Mulet X, Ho KK, Lossi N, et al. A small molecule inhibitor for phosphatase and tensin homologue deleted on chromosome 10 (PTEN). ACS Chem Biol 2006;1:780–790. [PubMed: 17240976]

40). Faucherre A, Taylor GS, Overvoorde J, Dixon JE, Hertog J. Zebrafish pten genes have overlapping and non-redundant functions in tumorigenesis and embryonic development. Oncogene 2008;27:1079–1086. [PubMed: 17704803]

41). Sun H, Lesche R, Li D-M, Liliental J, Zhang H, Gao J, et al. PTEN modulates cell cycle progression and cell survival by regulating phosphatidylinositol 3,4,5,-trisphosphate and Akt/protein kinase B signaling pathway. Proc Natl Acad Sci U S A 1999;96:6199–6204. [PubMed: 10339565]

42). Huang X, Zeng Y, Wang X, Ma X, Li Q, Li N, et al. FXR blocks the growth of liver cancer cells through inhibiting mTOR-s6K pathway. Biochem Biophys Res Commun 2016;474:351–356. [PubMed: 27109477]

43). Yang L, Miao L, Liang F, Huang H, Teng X, Li S, et al. The mTORC1 effectors S6K1 and 4E-BP play different roles in CNS axon regeneration. Nat Commun 2014;5:5416. [PubMed: 25382660]

44). Meng Z, Wang Y, Wang L, Jin W, Liu N, Pan H, et al. FXR regulates liver repair after CCl4-induced toxic injury. Mol Endocrinol 2010;24:886–897. [PubMed: 20211986]

45). Xie Y, Wang H, Cheng X, Wu Y, Cao L, Wu M, et al. Farnesoid X receptor activation promotes cell proliferation via PDK4-controlled metabolic reprogramming. Sci Rep 2016;6:18751. [PubMed: 26728993]

46). Liu X, Zhang X, Ji L, Gu J, Zhou M, Chen S. Farnesoid X receptor associates with beta-catenin and inhibits its activity in hepatocellular carcinoma. Oncotarget 2015;6:4226–4238. [PubMed: 25650661]

47). Modica S, Murzilli S, Salvatore L, Schmidt DR, Moschetta A. Nuclear bile acid receptor FXR protects against intestinal tumorigenesis. Cancer Res 2008;68:9589–9594. [PubMed: 19047134]

48). Song MS, Salmena L, Pandolfi PP. The functions and regulation of the PTEN tumour suppressor. Nat Rev Mol Cell Biol 2012;13:283–296. [PubMed: 22473468]

49). He J, Chen J, Wei X, Leng H, Mu H, Cai P, et al. Mammalian target of rapamycin complex 1 signaling is required for the dedifferentiation from biliary cell to bipotential progenitor cell in zebrafish liver regeneration. Hepatology 2019;70:2092–2106. [PubMed: 31136010]

50). Planas-Paz L, Sun T, Pikiolek M, Cochran NR, Bergling S, Orsini V, et al. YAP, but not RSPO-LGR4/5, signaling in biliary epithelial cells promotes a ductular reaction in response to liver injury. Cell Stem Cell 2019;25:39–53.e10. [PubMed: 31080135]

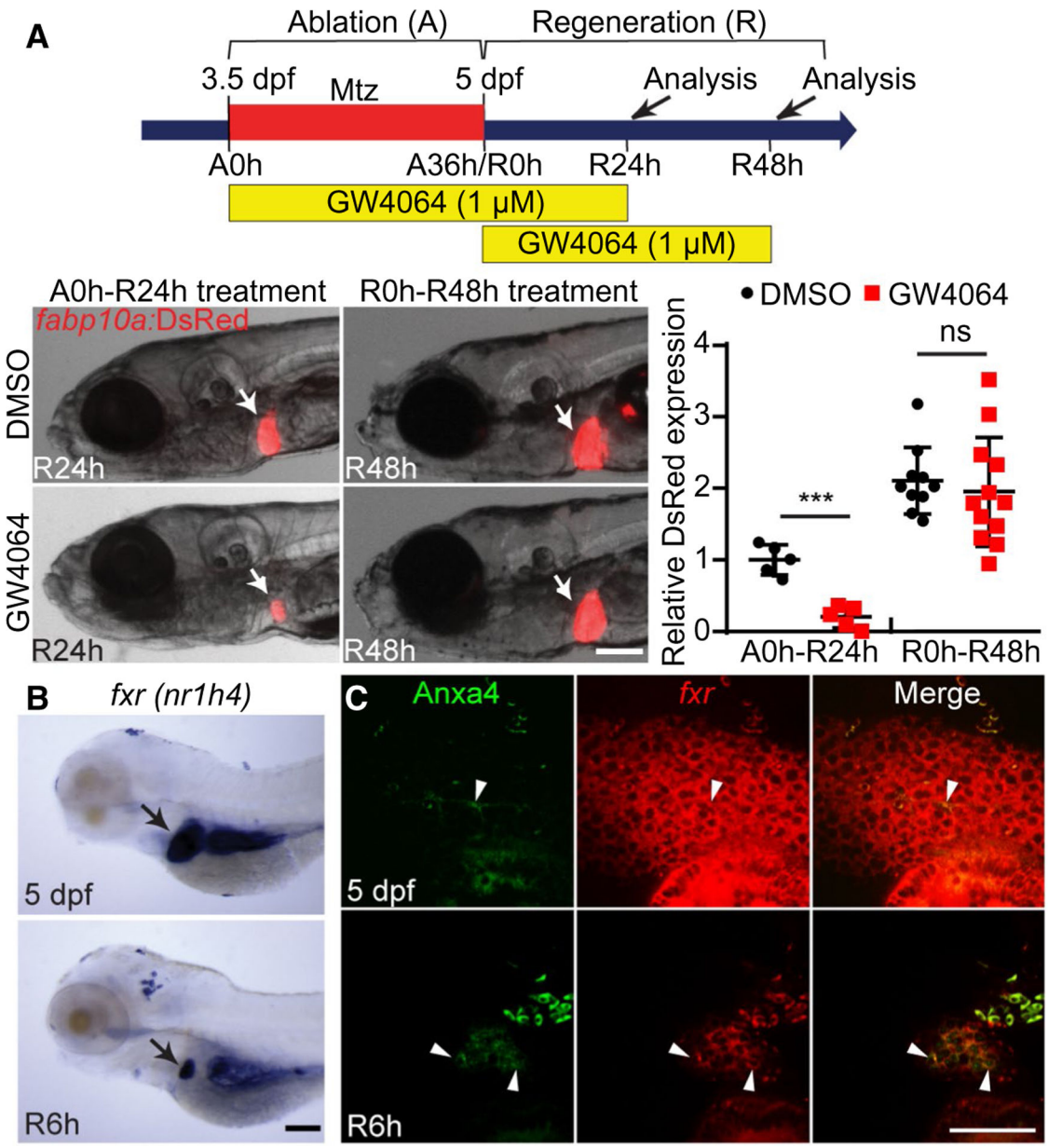

FIG. 1.

FXR activation impairs BEC-driven liver regeneration. (A) Epifluorescence images showing *fabp10a:*DsRed expression in regenerating larvae. Arrows point to the liver. Scheme illustrates the stages of Mtz and GW4064 treatment and analysis (arrows). Quantification of hepatic *fabp10a:*DsRed fluorescence in the regenerating larvae is shown. Data are presented as mean ± SEM. ***$P < 0.001$; statistical significance was calculated using an unpaired two-tailed *t* test. (B) Whole-mount *in situ* hybridization images showing hepatic *fxr* expression (arrows) in normal larvae at 5 dpf and regenerating larvae at R6h. (C) Confocal images showing *fxr* and Anxa4 expression in the liver. Arrowheads point to *fxr*/Anxa4 double-positive cells. Scale bars: 100 (B), 50 μm (C). Abbreviation: ns, not significant.

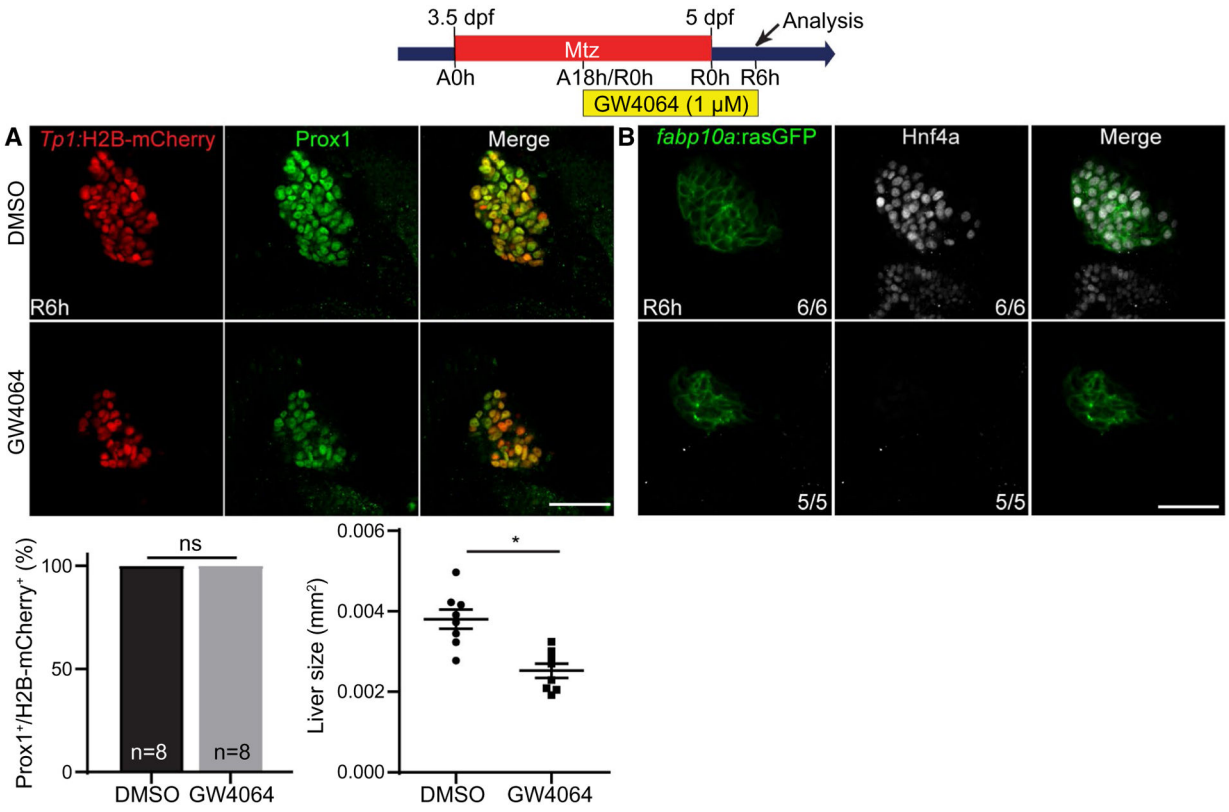

FIG. 2.

FXR activation does not block dedifferentiation of BECs into LPCs. (A) Single-optical section images showing the expression of Prox1 (green) and *Tp1:*H2B-mCherry (red) in regenerating livers at R6h. Quantification of the percentage of Prox1$^+$ among *Tp1*:H2B-mCherry$^+$ cells and liver size is shown. Data are presented as mean ± SEM. **P* < 0.05; statistical significance was calculated using an unpaired two-tailed *t* test. (B) Single-optical section images showing the expression of *fabp10a:* rasGFP (green) and Hnf4a (gray) in regenerating livers at R6h. Numbers in the lower-right corner indicate the proportion of larvae exhibiting the phenotype shown. Scale bars, 50 μm.

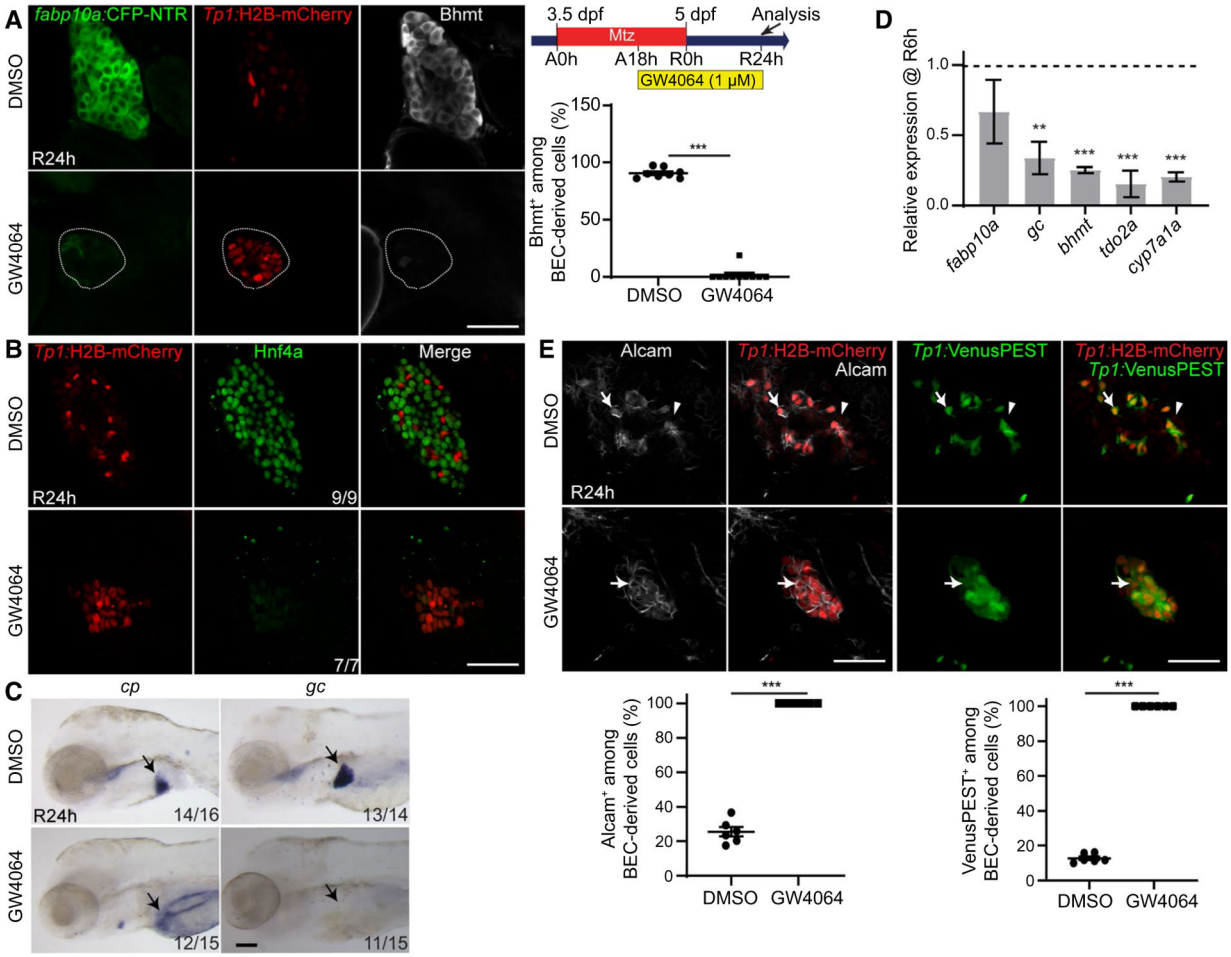

FIG. 3.

FXR activation blocks differentiation of LPCs into hepatocytes. (A) Single-optical section images showing the expression of *fabp10a*:CFP-NTR (green), Bhmt (gray), and *Tp1*:H2B-mCherry (red) in regenerating livers (dotted lines) at R24h. Quantification of the percentage of Bhmt^{+} (hepatocytes) among BEC-derived cells is shown. (B) Single-optical section images showing the expression of *Tp1*:H2B-mCherry (red) and Hnf4a (green) in regenerating livers at R24h. (C) Whole-mount *in situ* hybridization images showing *cp* and *gc* expression (arrows) in regenerating livers at R24h. Numbers in the lower-right corner indicate the proportion of larvae exhibiting the phenotype shown. (D) Quantitative PCR data showing the relative expression levels of *fabp10a, gc, bhmt, tdo2a*, and *cyp7a1a* between DMSO-treated and GW4064-treated regenerating livers at R6h. (E) Single-optical section images showing the expression of *Tp1*:VenusPEST (green), *Tp1*:H2B-mCherry (red), and Alcam (grey) in regenerating livers at R24h. Arrows point to *Tp1*:H2B-mCherry^{strong}/Alcam^{+} or *Tp1*:H2B-mCherry^{strong}/*Tp1*:VenusPEST^{+} cells (BECs or LPCs); arrowheads point to *Tp1*:H2B-mCherry^{weak}/Alcam^{-} or *Tp1:* H2B-mCherry^{weak}/*Tp1:*VenusPEST^{-} cells (hepatocytes derived from BECs). Quantification of the percentage of Alcam^{+} or VenusPEST among BEC-derived cells is shown. Data are presented as mean ± SEM. *$P < 0.05$, **$P < 0.01$, and ***$P < 0.001$; statistical significance was calculated using an unpaired two-tailed *t* test. Scale bars: 50 (A,B,E) and 100 μm (C).

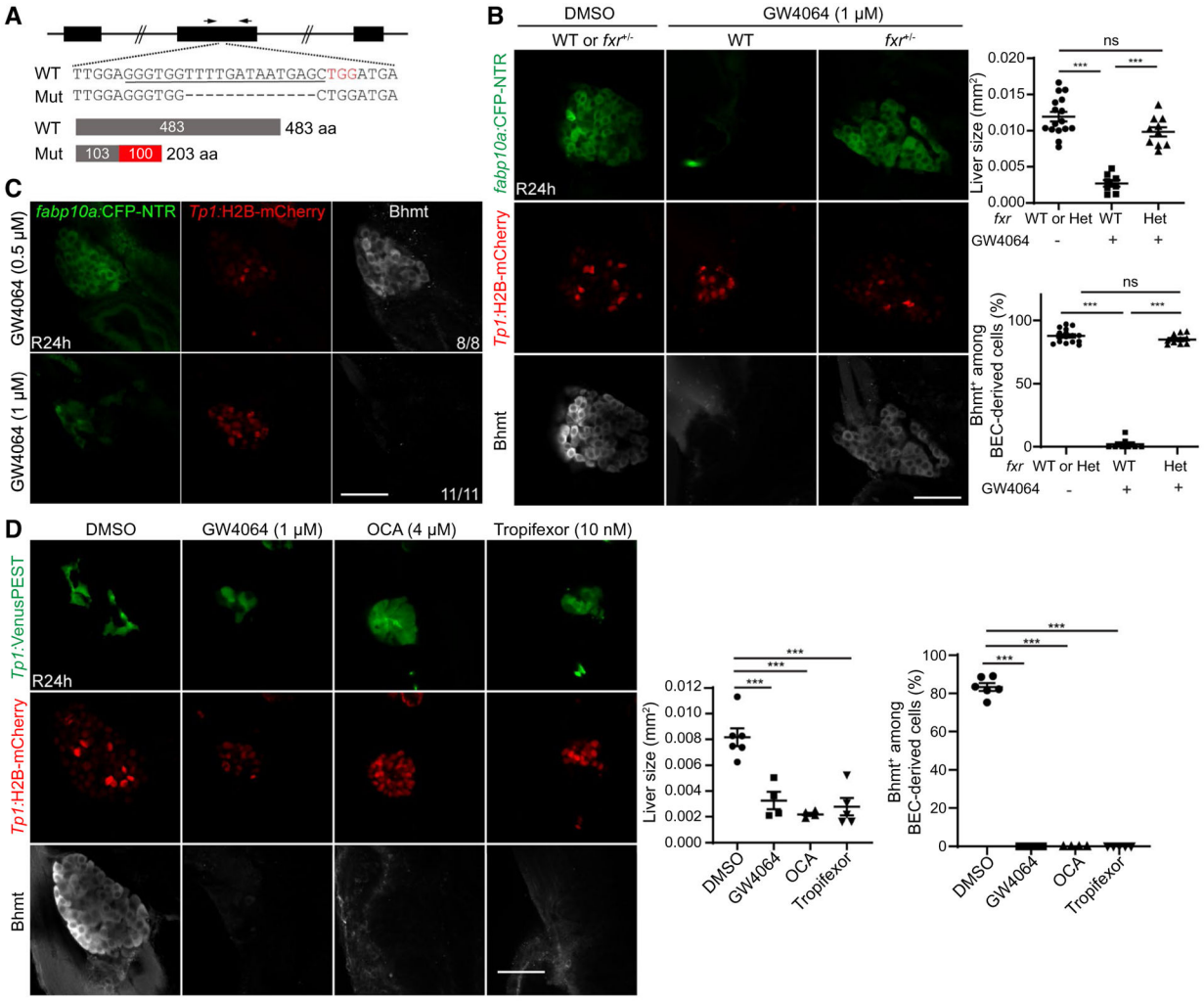

FIG. 4.

The effect of GW4064 on BEC-driven liver regeneration is mediated by FXR activation. (A) Scheme showing the deleted 13-base region in the *fx*r mutant allele. Its guide RNA target site is underlined; a protospacer adjacent motif sequence is marked in red. Arrows denote the regions of primers used for its genotyping. This frame-shift mutation produces a protein with 203 amino acids, of which 103 amino acids are from Fxr. (B) Single-optical section images showing the expression of *fabp10a*:CFP-NTR (green), *Tp1*:H2B-mCherry (red), and Bhmt (gray) in regenerating livers at R24h. Quantification of the percentage of Bhmt$^+$ among BEC-derived cells and liver size is shown. (C) Single-optical section images showing the expression of *fabp10a*:CFP-NTR (green), *Tp1*:H2B-mCherry (red), and Bhmt (gray) in regenerating livers at R24h. Numbers in the lower-right corner indicate the proportion of larvae exhibiting the phenotype shown. (D) Single-optical section images showing the expression of *Tp1*:VenusPEST (green), *Tp1*:H2B-mCherry (red), and Bhmt (gray) in regenerating livers at R24h. Quantification of the percentage of Bhmt$^+$ among BEC-derived cells and liver size are shown. Data are presented as mean ± SEM. ***$P <$ 0.001; statistical significance was calculated using one-way ANOVA. Scale bars: 50 μm. Abbreviation: WT, wild-type.

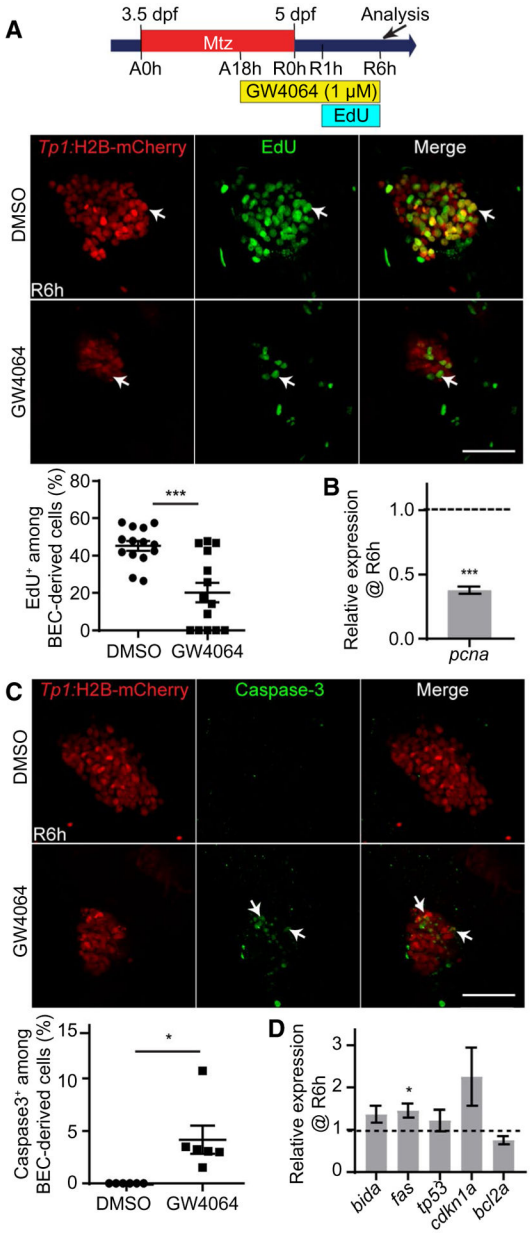

FIG. 5.

FXR activation reduces the proliferation of BEC-derived cells and increases their death. (A) Confocal images showing EdU (5-ethynyl-2′-deoxyuridine) labeling (green) and *Tp1:*H2B-mCherry expression (red) in regenerating livers at R6h. EdU was treated for 5 hours from R1h. Arrows point to EdU/H2B-mCherry double-positive cells. Quantification of the percentage of EdU^+ among BEC-derived cells is shown. (B) Quantitative PCR data showing the relative expression level of *pcna* (proliferating cell nuclear antigen) between DMSO-treated and GW4064-treated regenerating livers at R6h. (C) Confocal images showing the expression of *Tp1:*H2B-mCherry (red) and active Caspase-3 (green) in regenerating livers at R6h. Arrows point to Caspase-3/H2B-mCherry double-positive cells. Quantification of the percentage of Caspase-3 among BEC-derived cells is shown. (D) Quantitative PCR

data showing the relative expression levels of *bida, fas, tp53, cdkn1a*, and *bcl2a* between DMSO-treated and GW4064-treated regenerating livers at R6h. Data are presented as mean ± SEM. $*P < 0.05$ and $***P < 0.001$; statistical significance was calculated using an unpaired two-tailed *t* test. Scale bars: 50 μm.

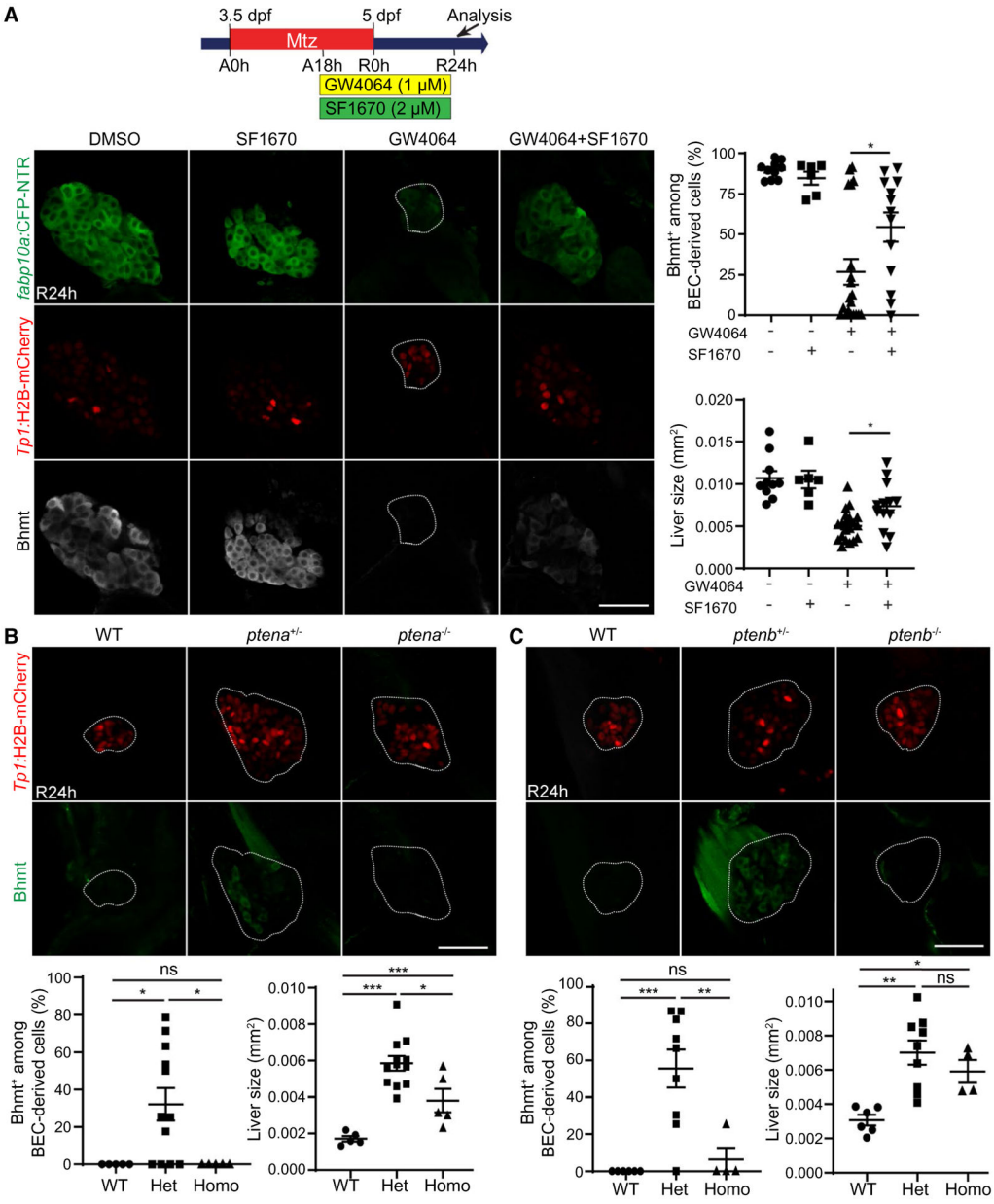

FIG. 6.

PTEN suppression rescues defects in BEC-driven liver regeneration observed in GW4064-treated regenerating larvae. (A) Single-optical section images showing the expression of *fabp10a*:CFP-NTR (green), *Tp1*:H2B-mCherry (red), and Bhmt (gray) in regenerating livers at R24h. Scheme illustrates the stages of Mtz, GW4064, and SF1670 treatments. (B,C) Single-optical section images showing the expression of *Tp1*:H2B-mcherry (red) and Bhmt (green) in regenerating livers at R24h. Dotted lines outline the liver. Quantification of the percentage of Bhmt^{+} among BEC-derived cells and liver size is shown. Data are presented as mean ± SEM. *$P < 0.05$, **$P < 0.01$, and ***$P < 0.001$; statistical significance was calculated using one-way ANOVA. Scale bars: 50 μm. Abbreviation: WT, wild-type.

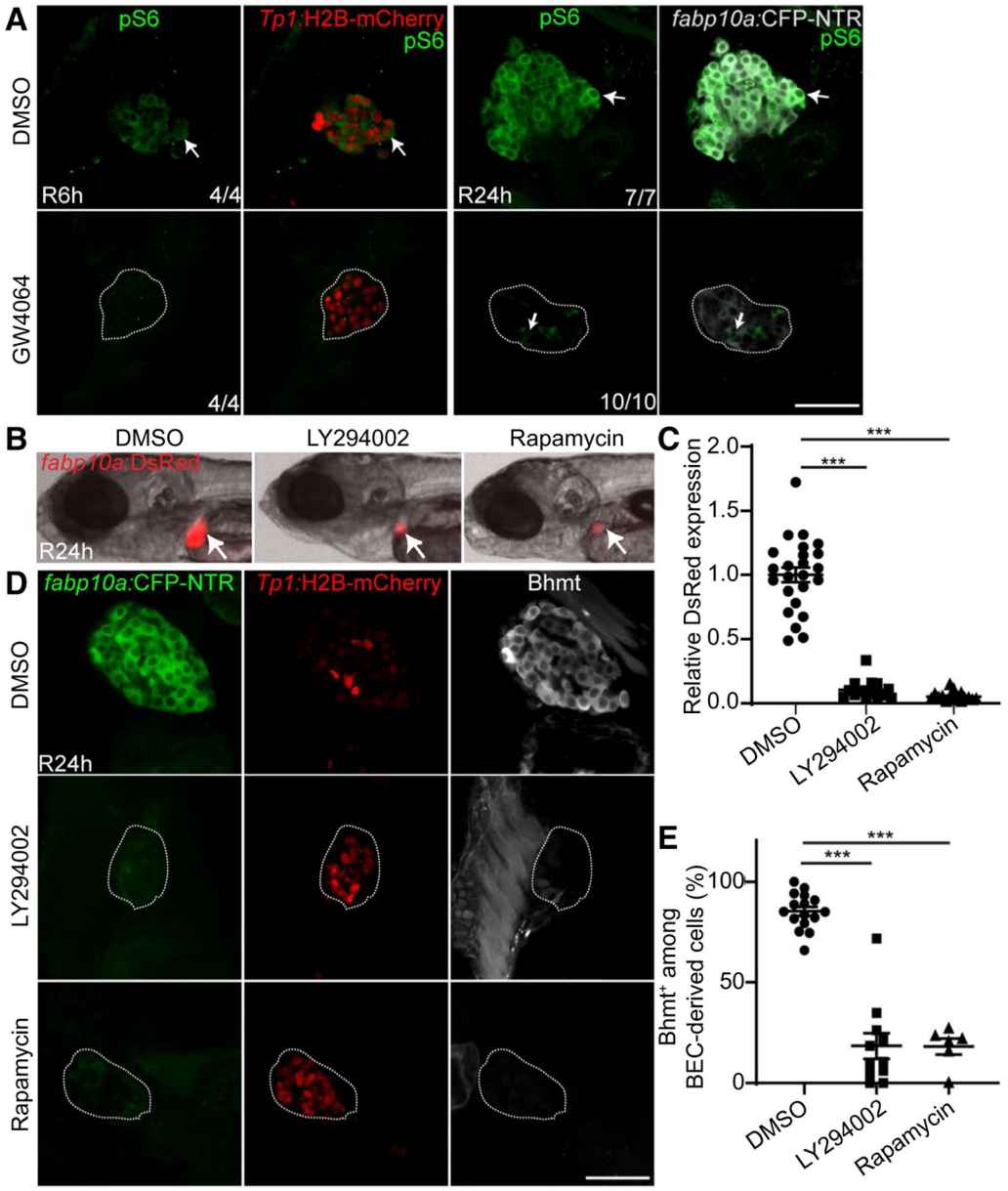

FIG. 7.

Inhibition of PI3K and mTOR signaling impairs BEC-driven liver regeneration, as does FXR activation. (A) Single-optical section images showing the expression of pS6 (green) and *Tp1*:H2B-mCherry (red) or *fabp10a*:CFP-NTR (gray) in regenerating livers at R6h or R24h. Arrows indicate pS6^{+} cells. Numbers in the lower-right corner indicate the proportion of larvae exhibiting the expression shown. (B) Epifluorescence images showing *fabp10a:*DsRed expression in regenerating larvae. Arrows point to the liver. (C) Quantification of hepatic *fabp10a:*DsRed fluorescence in the regenerating larvae shown in (B). (D) Single-optical section images showing the expression of *fabp10a*:CFP-NTR (green), *Tp1*:H2B-mCherry (red), and Bhmt (gray) in regenerating livers at R24h. Dotted lines outline the liver. (E) Graph showing the percentage of Bhmt^{+} among BEC-derived cells

shown in (D). Data are presented as mean ± SEM. ***$P < 0.001$; statistical significance was calculated using one-way ANOVA. Scale bars: 50 μm.